Cement and Concrete Research 40 (2010) 1327–1340

Contents lists available at ScienceDirect

Cement and Concrete Research

journal homepage: http://ees.elsevier.com/CEMCON/default.asp

Physico-chemical investigation of clayey/cement-based materials interaction in the context of geological waste disposal: Experimental approach and results

A. Dauzeres [a,b,*], P. Le Bescop [a], P. Sardini [b], C. Cau Dit Coumes [c]

[a] CEA Saclay, DEN, DANS, DPC, SCCME, Laboratoire d'Etude des Bétons et des Argiles, bât. 158, 91191 Gif sur Yvette, France
[b] Laboratoire HYDRASA FRE 3114 Université de Poitiers, bât. sciences naturelles, 86000 Poitiers, France
[c] CEA Marcoule, DEN, DTCD, SPDE, Laboratoire d'Etude de l'Enrobage des Déchets, bât. 438, 30207 Bagnols-sur-Cèze, France

ARTICLE INFO

Article history:
Received 25 May 2009
Accepted 17 March 2010

Keywords:
Characterization (B)
Waste management (E)
Interfacial transition zone (B)
Carbonation (C)

ABSTRACT

Within the concepts under study for the geological disposal of intermediate-level long-lived waste, cement-based materials are considered as candidate materials. The clayey surrounding rock and the cement-based material being considered differ greatly in their porewater composition. Experiments are conducted on the diffusion of solutes constituting those porewaters in a confined clay/cement composite system using cells. The test temperature was set at 25 °C and 2, 6 and 12 months. Results supply new information: carbonation is low and not clog the interface. Such absence of carbonation allows for the diffusion of aqueous species and, thus, for the degradation of the cement paste and the illitisation of illite/smectite interstratifications. The cement material is subjected to a decalcification: portlandite dissolution and a CaO/SiO_2 reduction in the calcium silicate hydrate. The sulphate in diffusion induces non-destructive ettringite precipitation in the largest pores. After 12 months, about 800 μm of cement material is concerned by decalcification.

1. Introduction

Current options for the geological disposal of intermediate-level long-lived waste (ILLW), as developed by the French National Radioactive Waste Management Agency (*Agence nationale pour la gestion des déchets radioactifs* — Andra), include cement materials used in contact with the surrounding clay rock, a mudstone, at Bure (France). Cement and concrete may be used as suitable materials for containers, massive embedding, backfilling or engineered barriers. As for clay materials, they are generally used as filling materials in drifts, engineered barriers or massive support. Any combination of both materials has to abide by safety and durability rules over long timescales of several thousands of years. Those materials have to preserve their containment properties, despite the potential thermal-hydrodynamic and physico-chemical stress induced by the environmental context. The natural water contained in the porosities of the host rock will modify cement materials. The chemical composition of water changes in contact with the hydraulic binder and causes physico-chemical modifications in the clay. Based on that knowledge, materials may be degraded and permeability may increase. In order to estimate the evolution of the repository over time, it is necessary to identify the various physico-chemical transformations of the material at its interfaces. Studies were performed to characterise clay/concrete interactions. Modelling and experimental work dealt with three main topics: the impact of an alkaline plume on clay or clay rock; the physico-chemical evolution of concrete under clay–water solicitations and, the study of interfaces between materials.

After a detailed state of the art, this paper presents an innovative experimental device (described in Section 4) relying on interfaces between CEM I cement paste and mudstone. The goal is to perform a set of experiments at 25 °C over 2, 6 and 12 months, and to examine the interface of the composite in order to identify physico-chemical transformations. The evolution of cement materials is highlighted by identifying decalcification, sulphate-attack and carbonation mechanisms. Significant analytical means are used to detect secondary mineral precipitations (zeolites, tobermorite-like phases, etc.), as observed in the state of the art, in order to provide solid experimental results and to build robust predictive models.

2. State of the art

Within Phases I (1997–2000) and II (2000–2003) [1] of projects on the effects of cement on clay barrier performance (ECOCLAY), an experimental approach was used to analyse the effects of an alkaline plume induced by concrete on bentonite [2,3]. Two types of experiments were initiated. The first consisted in batch reactors in which a bentonite suspension was produced in an alkaline solution. The second relied on transport cells in which two different types of materials in contact (mortar and compacted bentonite) were exposed to a flow of alkaline solution. Those experiments were conducted at temperatures ranging from 25 to 200 °C. At the interface, zeolites, analcime and phillipsite were formed at high temperatures, whereas

* Corresponding author. CEA Saclay, DEN, DANS, DPC, SCCME, Laboratoire d'Etude des Bétons et des Argiles, bât. 158, 91191 Gif sur Yvette, France.
E-mail address: alexandre.dauzeres@cea.fr (A. Dauzeres).

0008-8846/$ – see front matter © 2010 Elsevier Ltd. All rights reserved.
doi:10.1016/j.cemconres.2010.03.015

magnesium-clay precipitated and tobermorite-type hydrated calcium silicate (C–S–H) gel was observed. Several *in-situ* studies were performed through experimental and simulation approaches: one dealt with the mineralogical modifications induced by Boom-clay/Portland cement interactions at different temperatures [4]. After 18 months, the depth of the degradation zone in the cement material was about 100–150 µm. That zone was characterised by portlandite dissolution and a porosity increase. The work emphasised the transfers of major elements, such as calcium, silicon, aluminium, iron and sulphur, in the degraded zone. The phases of precipitated minerals included magnesium-aluminate hydroxide, magnesium-silicate hydroxide and a low-crystallinity gel. A second *in-situ* study was carried out on clay/concrete interactions on the Tournemire Site, France [5]. Mineralogical characterisations by scanning electron microscopy (SEM) and X-ray diffraction (XRD) were performed on materials in contact for 7, 15 and 125 years. Within the saturated zone of the clay host rock, gypsum precipitation and the recrystallisation of mixed-layer clays were observed, as well as localised zeolites. Near the interface, chlorite and kaolinite were dissolved and severe dolomite dissolution occurred. The Tournemire clay rock, a mudstone, was used to carry out experiments in "batch reactors" [6]. Clay was used either in powder or in fragments. The material was put in contact with a hyperalkaline solution. Comparison was only possible between experiments over the short term. The mudstone contained pyrite and dissolved dolomite, as well as a calcium-carbonate (calcite) precipitate. Localised zeolites were spotted by SEM.

The concrete/clay interactions were mainly studied by observing the impact of an alkaline fluid, representing the porewaters of a cement material on a clay rock, a clay mineral or a clay soil. A large number of papers were produced. Thus, the impact of alkaline solutions (with a potential of hydrogen [pH] equal to 13.2) on the clay mineralogy of the Callovo–Oxfordian formation was studied at 60 °C in batch reactors [7]. The authors presented the smectite degradation and the precipitation of a tobermorite-like phase. Several experiments were performed on the Opalinus clay from Mont Terri, Switzerland, with different types of alkaline fluids: pH 13.2 (potassium, sodium, and calcium) at 30 °C [8], pH 13 and 12 with sodium hydroxide (NaOH) and potassium hydroxide (KOH) at high temperatures (150 to 200 °C) [9,10]. Zeolite-type analcime, phillipsite, rectorite-sodium and potassium were observed at high temperatures.

The identification of the rate and reaction mechanisms of silicate minerals (quartz, feldspars, micas and clays) with cement-pore fluids (sodium, potassium, and calcium) was investigated through a series of laboratory experiments at 70 °C [11]. Results point out a C–S–H precipitation. The rate of calcium–sulphur–hydrogen growths was limited by the dissolution of primary silicates supplying silicon. Followed by atomic force microscopy, the montmorillonite dissolution under alkaline conditions (pH = 13.3) at 30, 50 and 70 °C showed that the dissolution rates of individual particles were independent of particle morphology, size and stacking [12]. The evolution in the mineralogy of an alkaline flow rate through a sandstone column was studied [13]. The authors observed quartz and feldspar dissolutions, as well as phase precipitations for C–S–H and hydrated calcium alumino–silicate (C–A–S–H). A study dealt with smectite and kaolinite dissolution at 35 and 80 °C in potassium-hydroxide solutions (0.1–4 M) with different solid-mass/solution-volume ratios in batch reactors [14]. It underlined the difference of the dissolution rate between both minerals and explained that phenomenon by structural differences. After a full review of experimental and modelling studies about the expected interactions of alkaline fluids with 'host rocks' around radioactive waste repositories, a study presented experimental results about alkaline-fluid/mineral interactions (calcium-hydroxide solution/muscovite/chlorite) at 85 °C for 800 h [15]. Solids were analysed by analytical transmission electron microscopy (ATEM). It showed the formation of C–A–S–H phases and the precipitation of local zeolites. The impact of the circulation of a portlandite-saturated water on a mixture of compacted mudstone and sand or MX-80 for 3, 6 and 12 months at 20 and 60 °C was studied [16]. The porosity, before and after circulation was determined with mercury-intrusion porosimetry. The sand mixture was exposed to a low degradation, while the bentonite mixture was strongly degraded. Innovative work was performed on swelling bentonite exposed to a highly-alkaline fluid (pH>12) [17]. The swelling pressure of the bentonite was significantly reduced for solutions with a higher pH than 13, with higher sodium-hydroxide concentrations than 0.3 M, due to montmorillonite dissolution. The diffusion of alkaline cations, or the flow of alkaline fluids through clay materials and the effect of diffusion properties were widely studied [18,19]. An author examined the effect of various high pH solutions on sodium-calcium smectites at 150 °C for two months with a pH ranging between 10 and 12 [20]. The use of a potassium-hydroxide solution induced a significant replacement of sodium by potassium, and a partial substitution of calcium by potassium. In the presence of potassium carbonate (K_2CO_3), a part of sodium-calcium smectites were replaced by zeolites (merlinoite), feldspars and a C-S–H-type tobermorite-like phase. Quartz precipitation was observed at high temperatures. Other investigations were conducted on that topic, such as a study on montmorillonite dissolution in compacted bentonite, when exposed to an alkaline solution, and its impact on bentonite permeability [21]. A very interesting study was conducted about the impact of low-pH cement solutions on Friedland Ton (70% montmorillonite and 30% muscovite) [22]. Contrary to classical cement solutions (higher pH), a very small change in potassium content was generated by the low-pH cement solution, thus inducing an insignificant illitisation of Friedland Ton. The chemical behaviour of Callovo–Oxfordian clay from the Meuse/Haute Marne area, when exposed to an alkaline solution, was studied by XRD and a cationic-exchange-capacity (CEC) survey [23]. Through a closed-system experiment, a representative solution of CEM I material containing NaOH, KOH and calcium hydroxide ($Ca(OH)_2$) was tested at different temperatures (60–120 °C) and timescales (6–168 h). The main results show zeolite, tobermorite and katoite precipitated, whereas mica and chlorite remained unchanged, but smectite and illite–smectite interstratifications were strongly reactive. In conclusion, the authors suggested three different phyllosilicate-alteration reactions in relation to both pH and the chemical composition of the reacting solution: (1) at a pH of 10 or 12, the precipitation of the solution components (beidellitic phases + alkali silicates); (2) at a pH of 14 for NaOH and KOH, the precipitation of alkali silicates + amorphous phases, and (3) at a pH of 14 for a solution in equilibrium with portlandite, the precipitation of alkali silicates + amorphous phases. Other papers were prepared about the alteration of bentonite by alkaline fluids [24,25].

Two important reviews summed up all experiments carried out on the alkaline alteration of clay materials [26,27], with the second one underlining precisely the role of secondary minerals. The study listed the minerals that precipitated in the different experiments concerning bentonite/hyperalkaline-fluid interactions. C–S–H, C–A–S–H, zeolites, feldspars, hydroxides, carbonates, silica polymorphs constitute the potentially-identified products in cement–bentonite interactions.

The degradation of cement materials by clay solutions (groundwaters) has been less studied in the literature. A study was carried out the behaviour of CEM I cement paste in contact with a clay solution representative of the clay rock from the Callovo–Oxfordian formation [28]. The work underlined the inhibition of degradation processes (sulphate attack and leaching) associated with the exogenous calcite crust formation over the initial surface of the cement paste. Some experiments dealt with the alteration of cement materials by different waters [29–33]. Kurashige et al., in particular, have worked on hydrogenocarbonates and chloride-charged waters, observing the evolution of calcium leaching in comparison with the precipitation of calcium carbonate.

Several modelling studies were carried out on clay/concrete interactions, such as: (1) simulations on mudstone/concrete interfaces over the short term (15 years) [34] or the long term (100,000 years) [35] using HYTEC or ALLIANCES [36]; (2) simulations of an alkaline plume in a clay barrier using PHREEQC [37] or PRECIP [38] or KINDIS [39], and (3) modelling reactions between cement-pore solutions and a crystalline rock [40] or between a fractured marl and a high pH plume [41].

A very rich literature exists about the chemical behaviour of clay when exposed to an alkaline plume at low and very high temperatures. Experimental data are extensive and allow for building solid predictive models. The knowledge base is solid about the chemical mechanisms controlling the clay material in contact with an alkaline solution. Experimental options are varied: types of material, test temperatures, durations and solution types. The chemical behaviours observed are recurrent irrespective of the tests involved: smectite illitisation with KOH solution, C-S-H or C–A–S–H formation with solutions in equilibrium with $Ca(OH)_2$ and sometimes M–S–H formation. Zeolite precipitations are commonly observed with tests at high temperature or long term-experiments (several years). Those experiments are necessary to identify the chemical behaviour of clay under alkaline conditions. But those tests are simplified tests for clay/concrete interactions. The real volumes of solutions contained in the porosities of the materials compare to those of solid surfaces, and volumes are not taken into account. The representative tests with clay/concrete interfaces are inescapable to understand the physico-chemical mechanisms.

If several models exist concerning the behaviour of cement when exposed to a clayey environment, representative experimental data are very scarce and prevent any validation of evolution models. Some experimental work carried out about the clay/concrete interface has been oriented on the degradation of clay material being considered as the "altered" material, and concrete as the "attacker". Only Read's work provides some data about the chemical behaviour of concrete: decalcification, magnesium and sulphur enrichment. The state of the art of cement material in contact with clay or argillite is very incomplete and requires special studies dedicated to the identification of physico-chemical mechanisms. Table 1 lists the published experiments relating to the alkaline alteration of clay materials and the clay/concrete interface.

3. Materials

Materials used in this study are Andra reference materials.

3.1. Clayey material

The clay rock, a mudstone, comes from Andra's Underground Research Laboratory (URL), straddling the Meuse and Haute Marne Departments, in France. Samples were collected at a depth of −490 m in the Callovo–Oxfordian formation. The mean mineralogical composition of mudstone is carbonates (23%), quartz (20%) + feldspars (2%), clay minerals (55%) and pyrite (<1%). The clay fraction is composed of chlorite, kaolinite (observed in trace at −490 m), illite, smectite and a mixed layer of clay and illite/smectite (I/S). In such an experiment, remoulded and compacted mudstone was used because the mechanical resistance of the rock is unsuitable for preparing clay-rock discs. Furthermore, this reworked and compacted mudstone is envisaged as sound material for backfilling drifts. The mineralogical composition of the remoulded mudstone is similar to that of the intact core. Fragments of retrieved cores were crushed with a ring-crusher, and the resulting powder was sifted at 250 µm (clay fraction is not impacted) and placed in a rubber membrane. A 60-MPa hydrostatic pressure was imposed on the powder in order to produce a compacted clay-rock cylinder. The last step consisted in preparing a cylinder measuring 42 mm in diameter and 5 mm in thickness. Characterisations were performed on the powder and on the final disc. XRD was used to determine the initial mineralogical components of the material (Fig. 1). Mercury-intrusion-porosity (MIP) tests, hydraulic conductivity and initial saturation-state calculations were performed (Table 2). Hydraulic conductivity was directly measured in the transport cell using the protocol presented below (Section 4.2).

3.2. Cementitious materials

The cement used is a sulphate-resisting Portland Cement (SRPC) CEM I, provided by Lafarge (Val d'Azergues), whose composition during the chemical and normative phases is detailed in Table 3.

Various sets of cement paste were prepared at a 0.4 water to cement ratio and cured for 3 months. Samples were placed in plastic bags in order to preserve the pore solution and to avoid carbonation. Cylinders with a 42-mm diameter were made for experimental purposes in transport cells. Many characterisations were carried out on the initial (non-degraded) cement paste. XRD analyses showed the initial mineralogy of the cement paste (Fig. 2). Mercury porosity, water porosity, hydraulic conductivity and initial saturation were measured (Table 4). The protocol based on the French Association of Research and Testing on Materials (*Association française de recherche et d'essai sur les matériaux* — AFREM) allowed for determining water porosity (ϕ) (Eq. 1) and the initial saturation state (Eq. 2). The following formulae were used to determine those values:

$$\phi = \frac{\left(m_{sat}^{air} - m_{dry}\right)}{\rho.V} = \frac{\left(m_{sat}^{air} - m_{dry}\right)}{\left(m_{sat}^{air} - m_{sat}^{w}\right)\rho} \quad \text{(Eq.1)}$$

$$m_{sl} = m_{dry} + \phi.sl.\rho \quad \text{(Eq.2)}$$

where m_{sl}, m_{sat}^{air}, m_{dry} and m_{sat}^{w} are the mass of the sample at saturation, at saturation weight at air, after drying (60 °C), and at saturation weight under water, respectively, whereas ρ is the water density.

The hydraulic conductivity was measured using an alkaline solution in the transport cell (see protocol in Section 4.2.).

4. Pore solutions

The exchange of soluble species impacts the evolution of mineralogy and induces changes in the porous medium. The knowledge of the initial pore solutions is important for understanding the geochemical reactions between cement paste and clay rock. Samples consisting of 250-mL cylinders were made to extract the pore solution. The extraction was performed with a press at a pressure ranging between 280 and 660 MPa. The recovered liquid volume was about 20 mL. The pH of the solution was measured with a pH electrode and the chemical composition was analysed by ionic chromatography (Table 5). It is worthwhile noting that the alkaline concentration was very high, with a potassium concentration of about 500 mmol L^{-1}.

The clay solution was not analysed in this study and the composition obtained from Ref. [58] was considered as a reference (Table 6). The solution contained a high bicarbonate (HCO_3^-) concentration. The partial pressure of carbon dioxide (pCO_2) in the Callovo–Oxfordian formation was 30 times higher than that in the atmosphere (25 °C). Those conditions favour carbonation. Concentrations of sulphates (SO_4^{2-}) and chloride (Cl^-) were higher than those in the cement-pore solution. The pH of the solution was 7.1.

4.1. Synthetic hyperalkaline solution

Only alkalis (K^+ and Na^+) were introduced in the solution. We suppose that, due to their low concentrations, Ca^{2+} and SO_4^{2-} will be in equilibrium with the cement material. In order to make a 100-mL

Table 1
Literature data summary concerning the clay/concrete interactions (clay alteration by alkaline solutions and clay/concrete interface experiments).

	Materials	Solutions	T (°C)	Times	Results	References
Bentonites	Na-bentonite	NaOH	20–85	3 to 12 months	Calcite precipitation and quartz dissolution at 85 °C after 3 months	[42]
	FEBEX	pH 10 to 13.5	35–60–90	7 to 365 days	Illite/smectite mixed-layer Illitization; Na-zeolites (analcime, phillipsite) precipitation + M–S–H or Mg-smectite. Primary compound dissolution	[43]
	FEBEX	NaOH 0.1 M–0.25 M–0.M + $Ca(OH)_2$	25–200	30 to 540 days	Phillipsite, analcime, saponite and tobermorite formation	[2]
	FEBEX	S1: pH 13.5; S2: $Ca(OH)_2$	25–60–90	2 to 268 days	With S1: merlinoite + chabazite at 60 °C and merlinoite at 90 °C. With S2: low evolution; equilibrium between C–S–H and montmorillonite at high temperature	[44]
	FEBEX	pH 13.5, NaOH + KOH	35–60–90	30 to 365 days	Na-phillipsite	[45]
	FEBEX (<2 μm)	pH 13.5, NaOH + CaO	60–90	30 to 90 days	Na-phillipsite + analcime	[45]
	MX-80	KOH (1 M)	60–90–120	1 to 7 days	Phillipsite	[46]
	MX-80	NaOH (1 M)	60–90–120	2 to 7 days	Analcime	[46]
	MX-80	CaO (0.5 M)	60–90–120	3 to 7 days	C–S–H gel + gypsum	[46]
	Bentonite + sand	pH 13 or 14 + NaOH	50–170	Up to 125 days	Time dependence for montmorillonite dissolution between 90 and 170 °C	[21]
Pure clay phases	Montmorillonite + kaolinite	$Ca(OH)_2$	25–50	5–125 min	Fast Ca(OH)2 adsorption	[47]
	Smectite	KOH	35–60	270 days	Illite/smectite formation	[48]
	Smectite	NaOH	35–60	270 days	Illite/smectite formation	[48]
	Smectite + kaolinite	KOH 4 M	35	–	Illite, phillipsite and K-feldspar formation	[14]
	Smectite + kaolinite	KOH 4 M	80	–	Strong illite formation and phillipsite and feldspar precipitations	[14]
	Na–Ca smectite	NaOH 0.1 M; pH 12	150	2 months	No evolution identified	[20]
	Na–Ca smectite	KOH + KCl 1M; pH 9.6	150	2 months	Interlayer substitution	[20]
	Na–Ca smectite	KOH + KCl 3M; pH 9.4	150	2 months	Interlayer substitution	[20]
	Na–Ca smectite	KOH + KCl 1M; pH 11.8	150	2 months	Illitization or beidellitization	[20]
	Na–Ca smectite	KOH + KCl 3M; pH 11.7	150	2 months	Illitization or beidellitization	[20]
	Na–smectite	K_2CO_3 2M; pH 11.7	150	2 months	Illitization or beidellitization + Na-merlinoite and Na-phillipsite	[20]
	Ca-smectite	K_2CO_3 2M; pH 11.7	150	2 months	Illitisation or beidellitisation + tobermorite type C–S–H	[20]
	Ca-montmorillonite	KOH 0.2 M	100–300	5–20 days	Illite, smectite, zeolite formations	[49]
	Smectite	NaOH 0.3 M	30–50–70	7 days	Smectite dissolution rate measurement under alkaline conditions	[12]
	Smectite	$Ca(OH)_2$ solution	–	Several months	Calcite formation	[50]
	Mg-smectite	NaOH solution	–	–	Brucite formation	[51]
	Montmorillonite	pH 1 à 13.5	25	–	Smectite dissolution rate measurements under acid and alkaline conditions	[52]
Clayey rocks	Opalinus clay	NaOH	150–175–200	50 days	Analcime, vermiculite, Na-rectorite	[9]
	Opalinus clay	KOH	150–175–200	50 days	Philipsite, K-feldspar, K-rectorite	[10]
	Opalinus clay	pH 13.2 with NaOH, KOH, $Ca(OH)_2$	30	540 days	Zeolites formation, C–A–S–H, dolomite dissolution, calcite, Fe-hydroxydes, syngenite	[8]
	Clashach sandstone	$Ca(OH)_2$ equilibrium	25	280 days	Quartz and feldspar dissolution, C–S–H precipitation	[13]
	Friedland clay	pH 9.4 and 8.1 (equilibrium with a low-pH cement)	–	5 months	No evolution. Low Illitization	[22]
	Tournemire argillite	pH 13	25–70	1 to 3 months	Dolomite and pyrite dissolution. Calcite precipitation	[6]
	Sandstone + clays + feldspars	$Ca(OH)_2$ solution	20–40	250 to 730 days	C–S–H and alkaline silica gels precipitation	[53]
	Maqarin biomicritic clays	Natural water hyperalkaline Ca–OH–SO_4 (pH>12.5)	–	100000 to 1 million years	C–S–H gels, ettringite and thaumasite precipitation	[54]
	Searles Lake clayey rock	Natural waters-low alcalinity (9<pH<10)	–	3 millions years	Smectite replacement (70%) by Fe-illite, analcime and K-feldspar precipitation	[55]
	Callovian–Oxfordian argillite	pH 13.2 (NaOH, KOH, $Ca(OH)_2$)	60	1 year	Smectite partial dissolution and illite. Microcrystalline quartz dissolution. Solubilization of organic matter. Tobermorite type C–S–H formation.	[7]
	Callovian–Oxfordian clays	NaOH, KOH, $Ca(OH)_2$	60–90–120	6, 24, 168 h	Analcime, chabazite, phillipsite, katoite and tobermorite formation. Smectite dissolution in illite/smectite mixed layer.	[23]
	Callovian–Oxfordian argillite	pH 12.7; Portland cement type solution	20	4 days	Alkaline solution impact on the organic matter compounds.	[56]

Table 1 (*continued*)

	Cement material	Clayey materials	T (°C)	Times	Cement material results	Clayey material results	References
Concrete/clay interface	CEM II concrete and silica CaO	Tournemire argilite	Variable	15 and 100 years	Carbonation (calcite/vaterite)	Gypsum, Na-zeolites, and dolomite formation, chlorite and kaolinite dissolution, Illite/smectite recrystallization with the CEM II concrete in contact	[5]
	CEM II concrete and silica CaO	Tournemire argilite	Variable	15 years	Carbonation (calcite/vaterite/aragonite)	Calcite/vaterite/aragonite	[57]
	CEM I mortar disc	FEBEX bentonite disc	25–60–120	1, 6 and 12 months	Alteration over few millimetres (convective experiments)	Alteration over few millimetres C–S–H gel and brucite formation at 25 et 60 °C. Strong degradation at 120 °C : tobermorite and Mg-saponite precipitation up to 10 mm and analcime (convective experiments)	[3]
	CEM I mortar disc	FEBEX bentonite disc	25–60–120	1, 6 and 12 months	Carbonation (convective experiments)	Analcime formation (convective experiments)	[2]
	7 cement paste: CEM I; CEM I + CV; CEM I + slags; cemented ion-exchange resins; high alumina cement; NIREX Reference Vault Backfill	Mol clays	25–85	12 to 18 months	Strong alteration: decalcification, S, Al, Si and Mg enrichment and precipitation of Si–Mg and Al–Mg gels near the interface.	Ca enrichment; Al, Si, Mg impoverishment.	[4]

hyperalkaline solution, 5 mL of NaOH 1-N solution and 95 mL of KOH 0.5-N solution were mixed in order to obtain 50 and 475 mmol L^{-1} for Na^+ and K^+ concentrations, respectively.

4.2. Synthetic clay solution

A two-step procedure was used to prepare a mudstone solution at 25 °C. Alkalis and alkali-earth mixtures were introduced in the form of sulphate, chloride and HCO_3^-. The main difficulty here was to obtain an equilibrium with the high pCO_2 being imposed [59,60]. When all species were dissolved, the pH was brought down to 7.1 by adding CO_2 gas. The method consisted in introducing potassium and calcium in the form of sulphate, as well as magnesium and strontium in the form of chlorides. Missing sulphate and chloride anions were added later together with sodium. Finally, a sodium complement was introduced in the form of bicarbonate. At that stage, the HCO_3^- concentration in the synthetic solution was about 2.89 mmol L^{-1} and the pH was equal to 8.5. In order to obtain 3.30 mmol L^{-1} of HCO_3^- concentration and a pH of 7.1, the acidity was fixed by a CO_2 partial pressure of ~1300 Pa in the gaseous volume of the reactor.

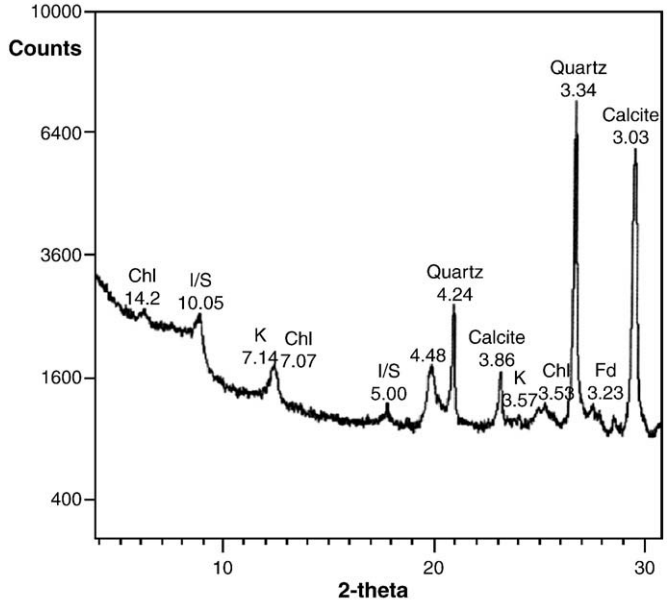

Fig. 1. XRD pattern of argilite powder <250 μm (Cu K-α, λ = 1.5405 Å) (Chl: chlorite, I/S: interstatified illite/smectite, K: kaolinite, Fd: K-feldspar).

5. Experiments

5.1. Principle of experiments in transport cells

Since clay-rock hydration induces swelling, the rock would quickly dislocate without the presence of any containment. For that reason, a transport cell, based on the Hoek cell was designed (Fig. 3). Hoek cells are commonly used to determine the elastic modulus and the strength of the rock under uniaxial and biaxial conditions.

Table 2
Physicals characteristics of remoulded clay rock.

Mercury porosity (%)	18
Hydraulic conductivity (m/s)	3.5×10^{-12}
Saturation (%)	60

Table 3
Cement composition (CEM I 52.5 N).

Chemical phase analysis [g/100 g]		Normative phase composition [g/100 g]	
CaO	65.1	Alite	65.4
SiO_2	20.9	Belite	13.6
Al_2O_3	3.2	Aluminate	0.9
Fe_2O_3	4.6	Ferrite	13.5
CaO (free)	1.8	Clinker	93.4
MgO	0.6	Gypsum	3.8
K_2O	0.6	Filler	2.8
Na_2O	0.1		
CO_2	1.1		
SO_3	2.76		

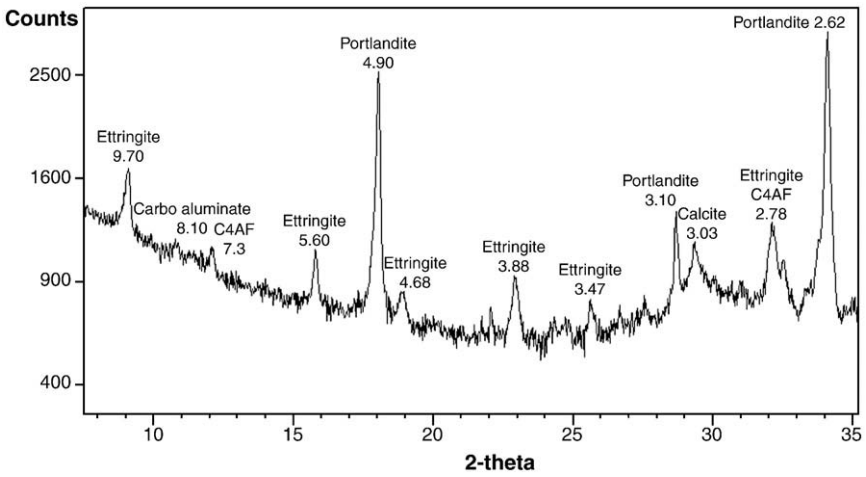

Fig. 2. XRD pattern of cement paste solid, w/c = 0.4 (Cu K-α, λ = 1.5405 Å).

In addition to the classical Hoek cell, an original hydration system was designed. Samples were vertically confined between upper and lower drilled pistons. A lateral containment was applied by an elastic membrane under water pressure provided by a Gilson® pump. The hydrostatic pressure, as applied on samples, was about 4 MPa at 25 °C. That device enabled hydration and a water-circulation pressure ranging between 0.5 and 2 MPa throughout the samples. Several floodgates were placed on the circuit. The hydration circuit was created in order to enable the use of the system in convective transport (open floodgates with an imposed pressure gradient) or in diffusive transport (closed circuit).

5.2. Protocol

Two independent cells were used to resaturate the cement paste and the compacted clay discs with a hyperalkaline solution and a clay solution, respectively. The resaturation of the cement paste is now described as a reference. The disc was placed in the elastic membrane of the cell, and the cell was filled with water. Pistons with porous plates were put in contact with the disc. Horizontal and vertical containment pressures were allowed in order to increase simultaneously and progressively with the final pressure ranging between 3 and 4 MPa. A hyperalkaline-solution flow, regulated by a Gilson pump, was applied on all samples. The resaturation time depended empirically on the thickness of the samples, applied pressure and the nature of the samples. A few tests were performed with a 15-mm-thick mudstone and a 20-mm-thick cement paste in order to estimate the optimal resaturation time. Figs. 4 and 5 show the relevant results for the resaturation times of a mudstone and a cement-paste disc, respectively. The flow rate was measured on a continuous basis at the outlet of the system. When the flow rate reached the steady state, the sample was considered to be resaturated (Figs. 4 and 5).

For cement paste (w/c = 0.4) and mudstone, the mean value of hydraulic conductivity was $3.5 \cdot 10^{-11}$ and $4 \cdot 10^{-12}$ m s^{-1}, respectively. Those values are consistent with those of previous studies [61,62]. The variations in permeability constitute the uncertainty resulting from the methodology of the experiment. When the discs were resaturated, the containment was removed from both cells. The cement paste was placed in contact with the saturated clay disc. After the confinement was applied, the clay/cement-paste composite evolved in diffusive mode in a closed system. No pressure gradient was applied through the composite. At the end of the experiment, containment stopped and the membrane was extracted with the composites. The discs were placed in a glove box under nitrogen atmosphere in order to prevent carbonation. Cutting operations and the first characterisations immediately began.

5.2.1. Analytical conditions

Multi-technical characterisations were used for solid analyses. First, a part of the clay/cement paste interface is embedded with an epoxy resin to maintain the sample during cutting. Second, the sample is cut into four parts: the first one (non-embedded solid sample) for XRD-characterisation purposes; the second (non-embedded thin section at the edge), for SEM purposes, the third (sample powder obtained by scratching the first non-embedded 100 µm layer) for solid nuclear-magnetic resonance (NMR) analytical purposes and the last embedded part for X-ray microtomography (prismatic sample of clay/concrete interface of 1.8 mm in height and 1-mm^2 section). XRD was used to characterise qualitatively the mineralogical evolutions of the solids. Data were collected using a PANalytical X'Pert diffractometer with an X'Celerator detector relying on CuKα radiation (λ = 1.5405 Å). The advantage of that detector is a reduction in the data-collection time by a factor of about 100 with no loss of resolution [63,64]. The working voltage and intensity were equal to 45 kV and 40 mA, respectively. The acquisition time of the XRD patterns shown in this paper was about 20 min. The clay sample was scanned between 4 and 65° and the cement sample between 5 and 60° with a step size

Table 4
Physical characteristics of cement paste (laboratory measurements).

Water porosity (%)	34
Mercury porosity (%)	25
Hydraulic conductivity (m/s)	4.10^{-11}
Saturation (%)	92

Table 5
Chemical composition of CEM I pore solution (28 and 90 days, w/c = 0.4).

Concentration (mmol L^{-1})						
Time	pH	[Na^+]	[K^+]	[Ca^{2+}]	[Cl^-]	[SO_4^{2-}]
28 days	13.60	47.4	452.4	0.8	1.4	5.6
90 days	13.64	50.4	474.2	1.6	0.6	6.7

Table 6
Chemical composition of the pore solution (25 °C) in the Callovo–Oxfordian (concentrations in mmol L^{-1}) [58].

T(°C)	Na	K	Ca	Mg	Sr	Cl	S	Si	Fe	Al	TIC*	pH
25	45.6	1.03	7.4	6.7	0.2	41.0	15.6	0.2	0.03	$4.7.10^{-6}$	3.3	7.1

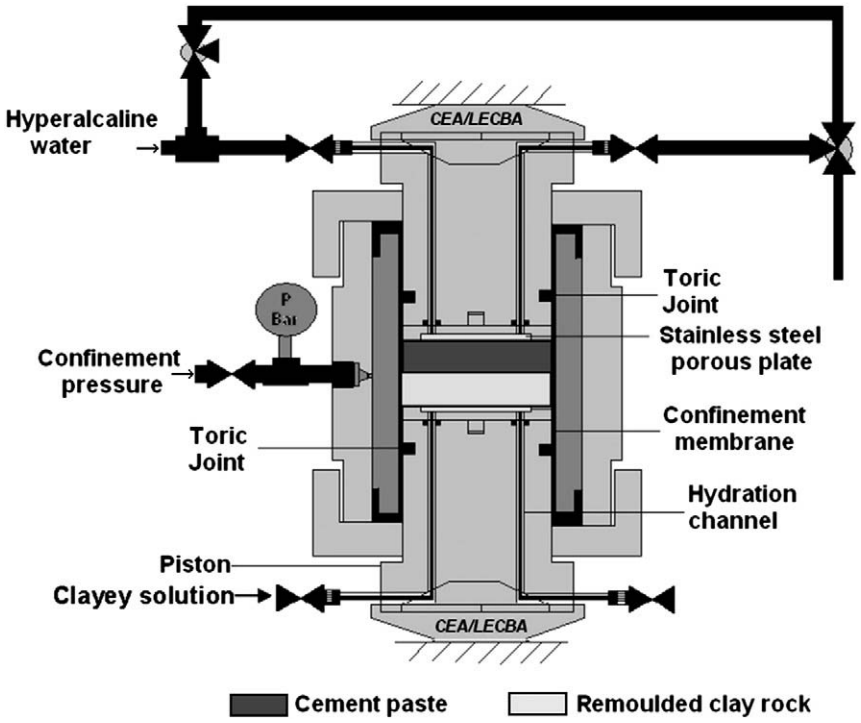

Fig. 3. Schematic view of the experimental transport cell.

of 0.017°. An XRD analysis was performed directly on the solid sample [65]. A first XRD pattern was drawn on the surface in contact with the clay rock. The surface was abraded over a depth of 10 µm (measured with a Mitutoyo absolute digimatic indicator) and the new surface was analysed. The abrasion was carried out with 350-grain abrasive paper. SEM characterizations were carried out with a FEG-SEM ULTRA 55 and a BRUCKER SDD detector containing ESPRIT software, under a working voltage of 15 KeV and a working distance of 16.5 mm for local chemical analysis. Observations were performed on a thin section cover by a thin carbon layer. The equipment used for NMR solids included a BRUCKER Avance 300 WB (magnetic field of 7 T (teslas). The powder intended for NMR analysis was placed in a rotor measuring 4 mm in diameter over a height of 18 mm. NMR measurements for ^{29}Si were recorded at a frequency of 59.29 MHz. The microtomograph being used was a *Skyscan 1172 High Resolution* (University of Jyväskylä, Finland), with a spatial resolution of 1 µm. The conditions of the X-ray tube were set in order to enhance the contrast between the different mineral components and the pores (100 kV, 100 mA). The angular step being used for radiography acquisition was 0.4° (acquisition time about 17 h). Image filtering, thresholding, and analysis were carried out with three imageing softwares: Micromorph™ for 2*D algorithmic tests, ImageJ and Aphelion™ for 3-D filtering and analysis tasks. Filtering and image segmentation were performed according to a simplified procedure, including the filtering of the original slices by a Gaussian kernel, and separated thresholding of open pores and porous zones according to upper and lower by boundaries. Three image-analysis routines were implemented slice by slice, each slice being parallel to the interface. Around the interface, the routines calculate the capillary-porosity profile (porosity>0.9 µm).

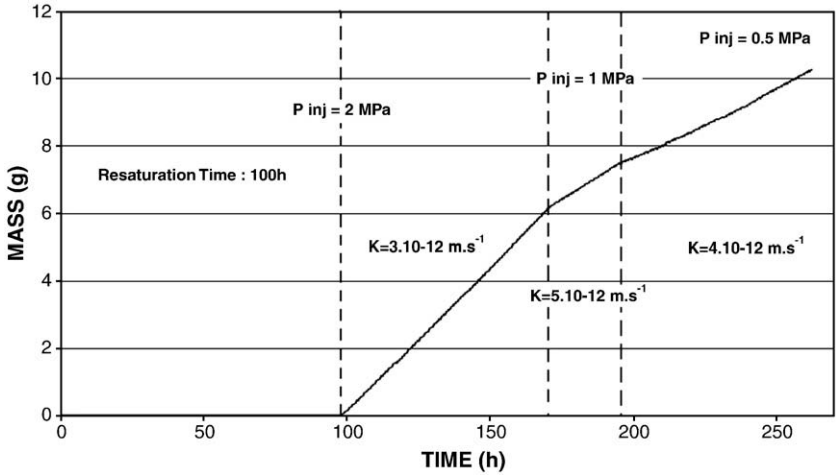

Fig. 4. Flow rate evolution and hydraulic conductivity calculation on compacted mudstone for different injection pressures (sample thickness = 15 mm).

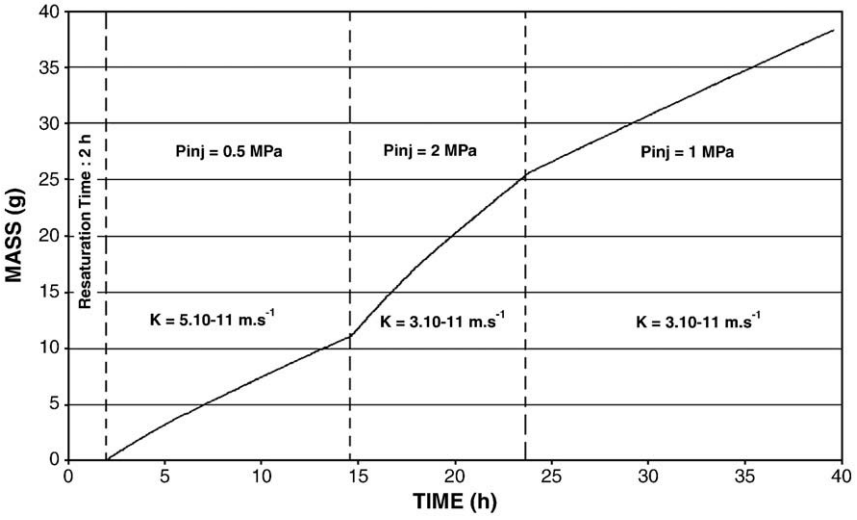

Fig. 5. Flow rate evolution and hydraulic conductivity calculation on cement paste CEM I, w/c = 0.4, for different injection pressures (sample thickness = 20 mm).

6. Results

Results presented in this paper deal with three experiments at 25 °C over 2, 6 and 12 months.

The first analyses performed refer to XRD. Various series of XRD patterns were performed from the surface deep into the cement-paste sample. Only a few selected diagrams are displayed to illustrate mineralogical evolutions. The XD patterns for cement-samples over the three time periods (2, 6 and 12 months) show systematically the following transformations: portlandite dissolution, ettringite precipitation and calcite precipitation. In relation to time, the portlandite dissolution, as identified by an evolution towards a 2.62-Å peak (Fig. 6a, b, c) indicates the progressive decalcification of the cement paste, with the thickness of those degradations reaching 200, 350 and about 800 µm after 2, 6 and 12 months, respectively. The sulphates originating from the clay solution generate the precipitation of ettringite. This paper shows the evolution towards a 9.70-Å peak (Fig. 6d, e, f). Those sulphate-attack phenomena increase with time the same way as the decalcification mentioned above. Maximum peak intensities occur in depth and not on the surface, where it is in contact with the clay material, and stand at 120, 210 and 100 µm after 2, 6 and 12 months, respectively. Carbonation was restricted to the first 5 or 10 µm and was not time-dependent (Fig. 6g, h, i).

Complementary analyses must be confronted in order to reach a satisfactory conclusion about the evolution of phenomena (SEM, NMR).

The decalcification of the cement material is confirmed by SEM analyses with EDS (Fig. 7) and ^{29}Si NMR results (Fig. 8). Several series of local chemical analyses were carried out in SEM-EDS on a thin section: (1) within the sound zone; (2) in the degraded zone for the 2, 6 and 12-month experiments. The silicon/calcium ratio is shown in relation to the aluminium/calcium ratio. The sound zone is characterised by the following system: ettringite, portlandite, C–S–H. The graph shows clearly a decrease in the CaO/SiO_2 ratio after 2 and 6 and 12 months of contact with the mudstone and a total portlandite dissolution. The degraded system is composed of ettringite and C–S–H with a CaO/SiO_2 ratio lower than that of the sound zone.

The C–S–H is the main component of the hydrated Portland cement paste. It was analysed accurately with the solid ^{29}Si NMR technique [66–69]. Q1 and Q2 types constitute silicon tetrahedrons of the end and middle chains, respectively. A high Q1/Q2 ratio means that C–S–H structures are characterised by short chains of silicon tetrahedrons and is typical of jennite structures with a high CaO/SiO_2 ratio [66]. A low Q1/Q2 ratio means that the C–S–H structures are characterised by long chains. That structure is representative of the tobermorite type with a low CaO/SiO_2 ratio [66]. C–S–H characterisations by solid-NMR were conducted on the initial cement paste and on the surface of the cement paste that was in contact with the mudstone for 2 and 12 months at a depth of 100 µm (Fig. 8).

The NMR spectrum of the initial cement paste shows the presence of residual belite (C2S). Q1-type silicone tetrahedrons appear more frequently than Q2-type ones, thus indicating that the CaO/SiO_2 ratio is high (Q1/Q2 = 1.5) in the C–S–H structures. After a two-month contact with the clay disc, the Q1/Q2 ratio fell considerably to 0.95 (estimated by simulation), thus proving that the CaO/SiO_2 ratio had also decreased. The depletion in calcium content in C–S–H phases may explain those observations. On the other hand, residual belite has also decreased: after a 12-month contact with mudstone, and the Q1/Q2 ratio fell down to 0.45. Those EDS analyses confirm the severe decalcification of the cement paste, as observed by XRD in the form of portlandite dissolution.

The direct determination of the CaO/SiO_2 ratio for C–S–H structures by NMR analyses is difficult. However, an estimation of the mean CaO/SiO_2 ratio of C–S–H structures is possible for low Q1/Q2 values (<0.8) [70]. After a 12-month contact, the mean CaO/SiO_2 ratio is estimated between 1 and 1.1.

For the mudstone contained in the composite, two major observations were formulated.

First, we observed transformations in the illite/smectite interstratifications. A series of XRD patterns on mudstone presents an increase in intensity to a 10-Å peak near the interface with the cement paste (Fig. 9a–b). The full width at half-maximum (FWHM) of the same peak decreased significantly in the interfacial zone over a depth of about 150–200 µm (Fig. 9b). Illite/smectite interstratifications present in the Callovo–Oxfordian formation are characterised by a peak of 10 Å (illite) and a shoulder around 11 Å (illite/smectite). That shoulder disappears with the degradation in the degraded zone and increases with the intensity of the illite peak. The FWHM analysis confirms that observation: only the illite peak remains and the FWHM decreases. Such illite enrichment was observed systematically in all experiments.

7. Discussion

7.1. Mineralogical and chemical evolutions

Porewater in mudstone is characterised by a neutral pH (7.1). The pore solution from the cement paste is in equilibrium with portlandite

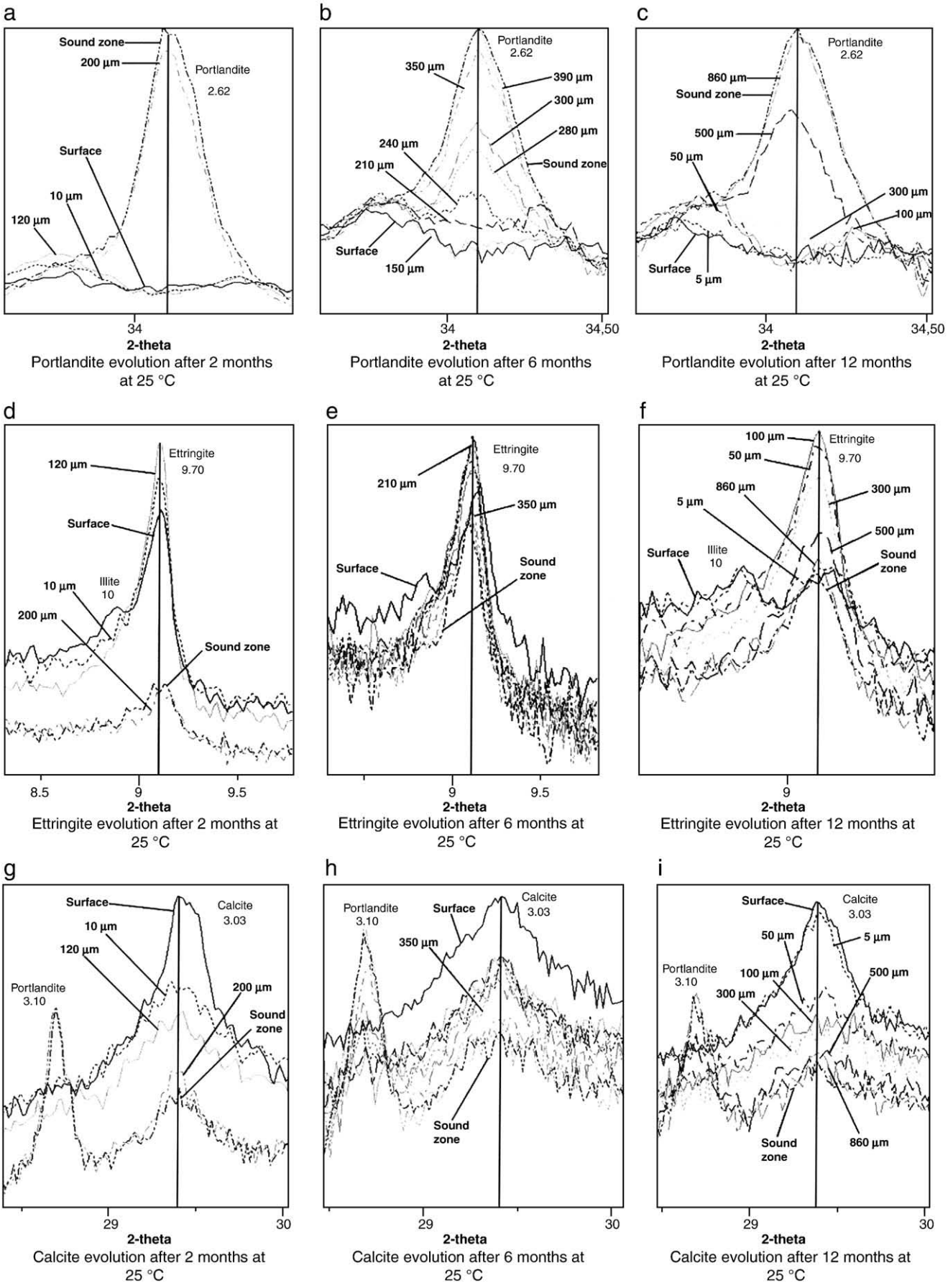

Fig. 6. Main mineralogical transformations identified by X-ray diffraction on cement pastes samples after a contact with mudstone at 25 °C during 2, 6 and 12 months.

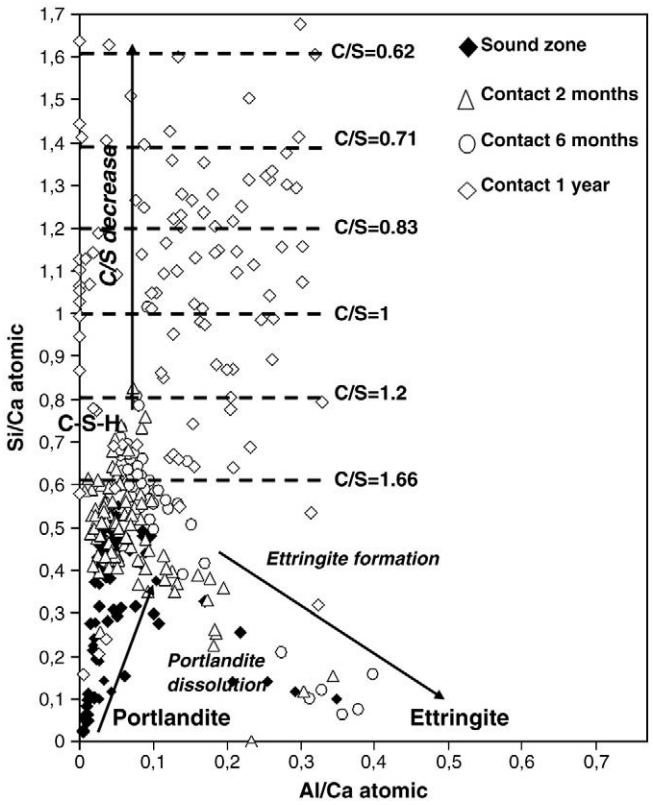

Fig. 7. Atom ratio plots of Si/Ca ratio vs. Al/Ca ratio for the matrix of cement paste in the sound zone and the degraded zone after 2, 6 months and 1 year of contact with mudstone.

and a high alkaline concentration imposing a pH equal to 13.6 at 25 °C. The penetration of the clay solution induces portlandite dissolution. Decalcification is also characterised by a CaO/SiO_2 decrease in C–S–H structures. Within the sound zone of the cement paste, the CaO/SiO_2 ratio is estimated to stand between 1.6 and 1.8. After being in contact with mudstone for 12 months, the mean value of the CaO/SiO_2 ratio is about 1.0. SEM analyses have shown that decalcification is not complete in the degraded zone. The portlandite is totally dissolved in that area over the three times, but C–S–H structures are not totally transformed into amorphous silica. That information is important in order to understand the evolution of the chemical system. Within the sound zone, the pH of the interstitial solution is controlled by the portlandite equilibrium and the high alkaline concentration (mainly potassium). The absence of potassium in the clay solution generates its leaching from the cement paste. That potassium associated with hydroxide ions is responsible for the evolution of the illite/smectite interstratifications in the mudstone. An illite enrichment is observed in the mudstone. That phenomenon in such context was described by Marty et al. [71]. After the alkaline leaching was completed in the cement paste, the pH was controlled by portlandite equilibrium (pH = 12.45 at 25 °C). Since portlandite had dissolved, the pH and the new chemical system were controlled by the C–S–H dissolution. The remaining C–S–H with a low CaO/SiO_2 ratio indicates that the pH in the degraded zone remains above 10 in the interstitial solution of the cement paste [72].

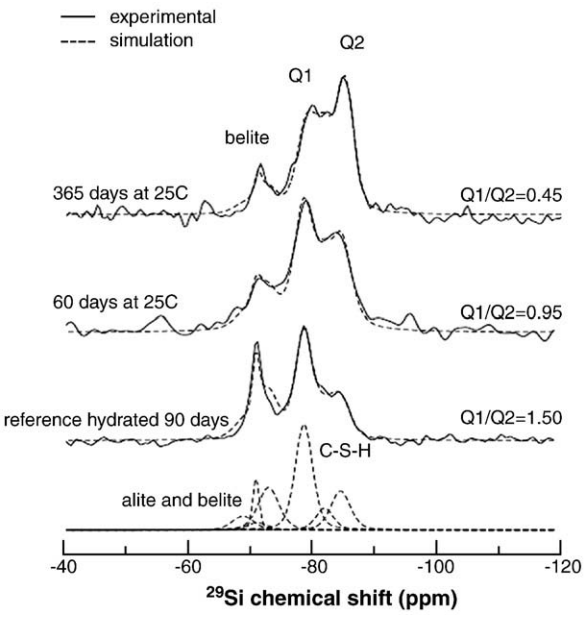

Fig. 8. ^{29}Si MAS NMR spectrum recorded by Solid Phase Extraction (SPE) at a spinning frequency of 15 kHz for the sound zone of CEM I cement paste, and the degraded zone of CEM I after a contact of 2 and 12 months with mudstone at 25 °C.

The pH evolution, the decalcification creating a calcium source, the high concentration in sulphates from mudstone and the system rich in aluminium cause the ettringite to precipitate and confirm the model exposed by Marty et al. [71]. After 12 months, ettringite is absent from the surface of the cement paste, but precipitates deep within the cement.

Carbonation, due to high HCO_3^- concentrations in the clay solution, causes calcite to precipitate to a limited thickness of 20 µm at the end of the 2, 6 and 12-months experiments.

7.2. Microstructure and degradation progress

Decalcification, mainly in the form of portlandite dissolution, provokes a porosity opening. Several simulations of clay/concrete interactions forecast calcium fixation by carbonation (calcite precipitation) [34,73]. In the case of CEM I cement paste in contact with underground water, carbonation induces the pores to clog [28,32] by the exogenous calcite crust formation. As a representative study of clay/concrete interactions, this study provides new information. Portlandite dissolution releases large quantities of calcium. A small part of that calcium is fixed by carbonation near the interface (calcite precipitation) and also by ettringite precipitation. The porosity openings associated with portlandite dissolution generate big cavities (up to 10 µm-thick) where needle-shaped ettringite is able to precipitate (Fig. 10). The silicon signal in the spectra corresponds to the C–S–H signal. This ettringite seems to be not destructive to the cement material. There is no obvious tendency to clog the interconnected network of macro-pores (Fig. 11).

Compared to the experiment in groundwaters [28,32], carbonation is very low and microstructures analysis does not show any clogging in the cement paste. The porosity which exceeds 1 µm, is characterised by X-ray Microtomography High Resolution and quantified by image analysis, is equal to 11% in the degraded zone against 1% in the sound zone of the cement paste. It is important to specify that the macroporosity is only a part of the overall porosity. However, the porosity profile shows a large zone of capillary-porosity opening, with a connected network, in relation with the portlandite dissolution thickness. The calcite not forms a crust, but heterogeneous precipitations over 20 µm in the cement paste. The following hypothesis is possible: the first portlandite crystals in contact with the mudstone are quickly dissolved and the calcium is immediately fixed by the local carbonates. Such precipitations reduce the local carbonate concentration. The portlandite continues to dissolve, but the carbonate flux is insufficient to induce significant calcite precipitation and a porosity clogging. The calcium is fixed by ettringite precipitation, diffuses into the mudstone or is probably partially sorbed by clay phases. For the time being, the latter issue has not been fully demonstrated yet.

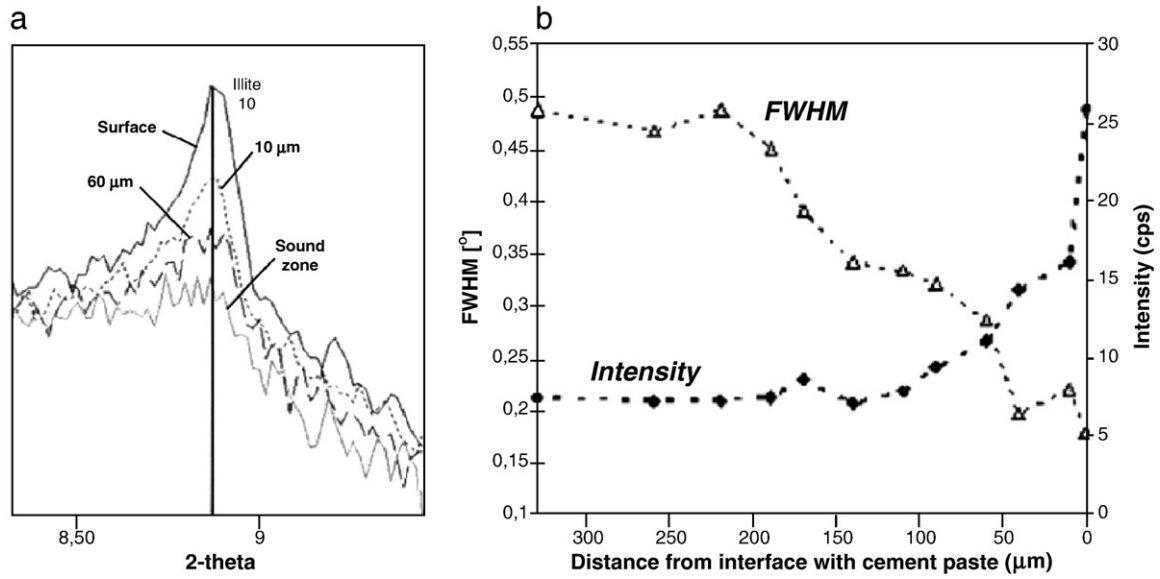

Fig. 9. a) XRD patterns of I/S zone of mudstone; b) profile of illite XRD intensities peaks with the depth compare to FWHM of the 10 Å peak; example of 2 months experiment in contact with mudstone at 25 °C.

The effect of such mineralogical changes on porosity has a substantial impact on the evolution of the degradation in the cement material. Degradation evolves rapidly (Fig. 12). Portlandite profiles suggest a proportional evolution to time (for experiments limited to 12 months): portlandite is totally dissolved at 200 and 400 µm after 6 and 12 months, respectively, whereas the sound zone is found at 400 and 800 µm at the end of the 6 and 12-month experiments, respectively.

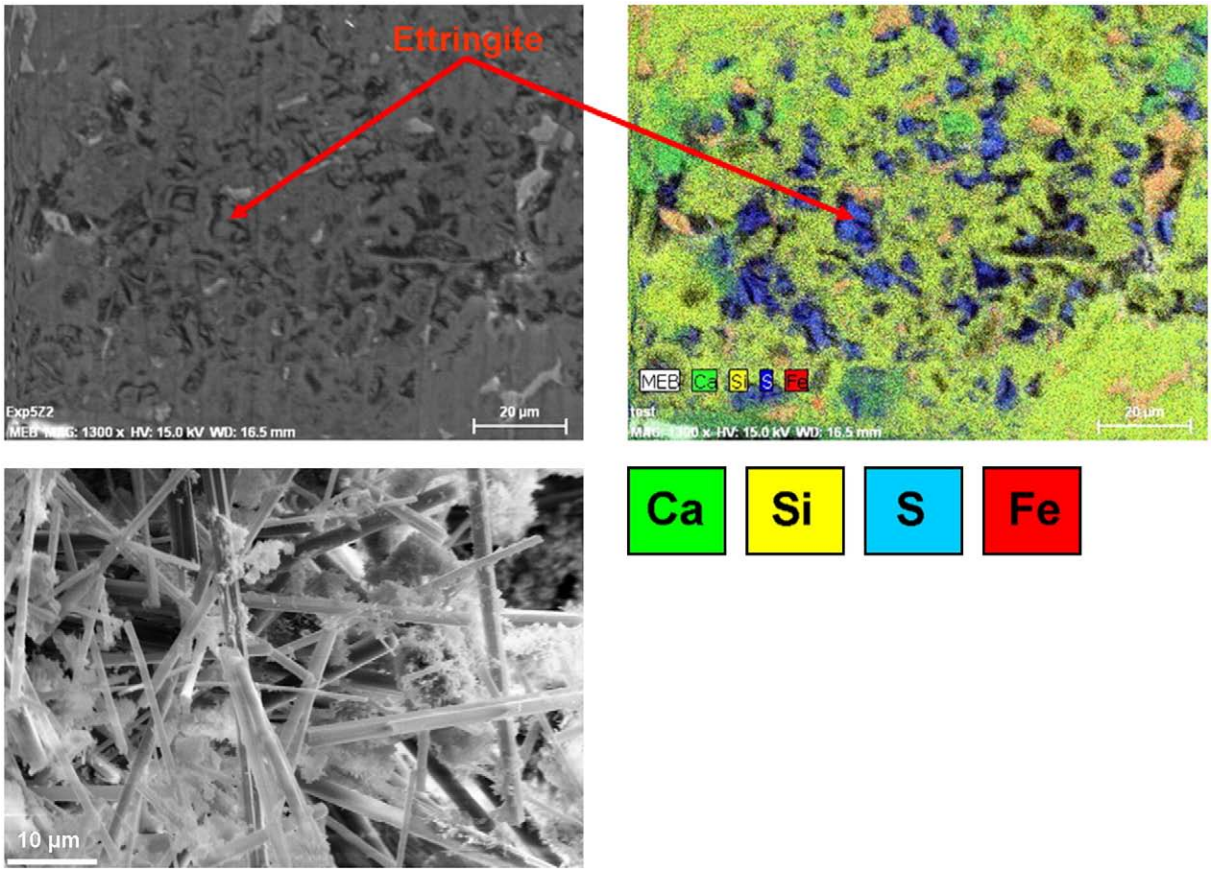

Fig. 10. SEM images and multi-elementary cartography of cement paste degradation zone; ettringite precipitation observed by SE mode.

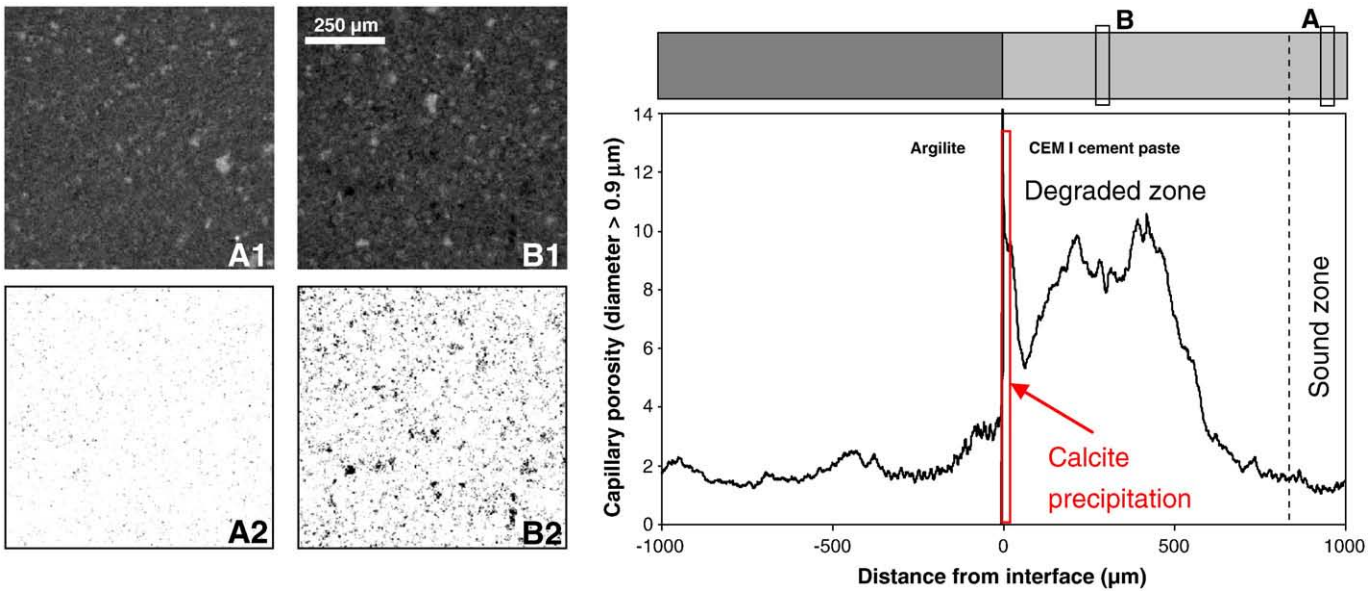

Fig. 11. Microtomography images of the sound zone (A1) and the surface in contact with the clayey rock (B1) of the cement paste after 1 year of interaction; porosity extraction by image analysis on the sound zone (A2) and the degraded zone (B2); macroporosity profile calculated by image analysis.

8. Conclusion

The studies about clay/alkaline-solution interactions are numerous (experiments, models) and the data about the evolution of the clay material are rich and varied. However, representative studies of clay/concrete interfaces are very scarce, and experimental data about cement behaviour in that context are poor. This paper presents an innovative experiment, in which CEM I cement paste and Bure mudstone is considered as a composite assemblage. This study provides new facts for understanding the system. First, the degradation of the cement paste is fast and, for short timescale, evolves in proportion with time. That evolution must be linked to pore openings due to portlandite dissolution and to the absence of pore clogging (due to very low carbonation). Part of the calcium is fixed as a result of ettringite precipitation in the portlandite-dissolution zone. Low carbonation is only present on the surface of the cement paste. The evolution of the chemical system may be described by the mineralogical-assemblage series. The sound zone is composed of C–S–H, ettringite and portlandite, with the latter imposing a pH of 12.45. The degraded zone is composed of ettringite and C–S–H (CaO/SiO_2 between 1.0 and 1.7) with the surface of cement paste composed only of C–S–H (CaO/SiO_2: 1.0–1.1) and calcite, where the pH lies between 10 and 11. The potassium plume resulting from the cement paste induces an illite enrichment within illite/smectite interstratifications.

Any future modelling work could consider those new experimental results, mainly macroporosity openings and the absence of clogging, thus inducing the degradation of a CEM I cement paste, in order to simulate representative evolutions of argillite/CEM I concrete interactions at 25 °C.

Acknowledgments

The authors wish to thank Andra for its financial support, as well as Drs. F. Brunet, M. Schlegel from the CEA and J. Timonen and M. Voutilainen from the University of Jyvaskyla for their valuable help and advice. All critical reviews and comments in the preparation of this paper are gratefully acknowledged.

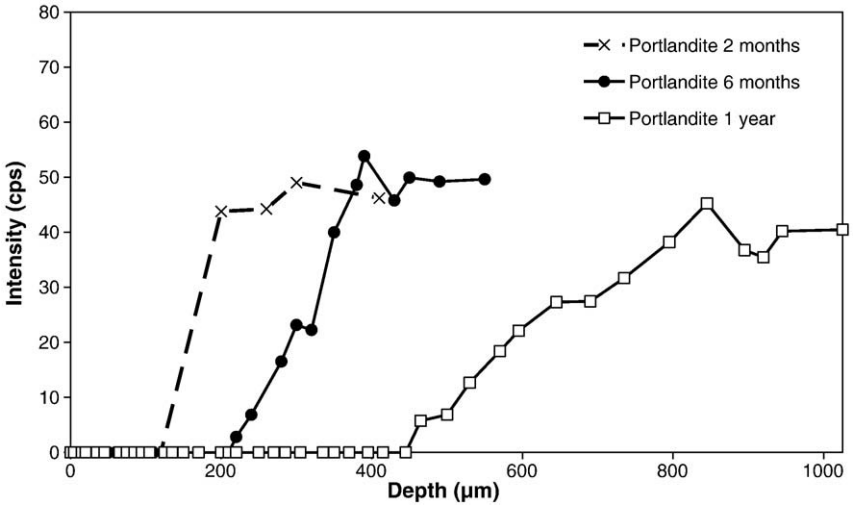

Fig. 12. XRD profile of portlandite in the CEM I cement paste after 2, 6 and 12 months of contact with the mudstone (qualitative method).

References

[1] N. Michau, Ecoclay II: Effect of cement on clay barrier performance phase II. Final report. European contract FIKW-CT-2000-00028, Andra ed, 2003.
[2] J. Cuevas, R. Vigil De La Villa, S. Ramirez, L. Sanchez, R. Fernandez, S. Leguey, The alkaline reaction of FEBEX bentonite: a contribution to the study of the performance of bentonite/concrete engineered barrier systems, Journal of Iberian Geology 32 (2) (2006) 151–174.
[3] R. Fernandez, J. Cuevas, L. Sanchez, R.V. de la Villa, S. Leguey, Reactivity of the cement–bentonite interface with alkaline solutions using transport cells, Applied Geochemistry 21 (2006) 977–992.
[4] D. Read, F.P. Glasser, C. Ayora, M.T. Guardiola, A. Sneyers, Mineralogical and microstructural changes accompanying the interaction of Boom Clay with ordinary Portland cement, Advances in Cement Research 13 (2001) 175–183 N°4, October.
[5] E. Tinseau, D. Bartier, L. Hassouta, I. Devol-Brown, D. Stammose, Mineralogical characterization of the Tournemire argillite after in situ interaction with concretes, Waste Management 26 (2006) 789–800.
[6] I. Devol-Brown, E. Tinseau, D. Bartier, D. Mifsud, D. Stammose, Interaction of Tournemire argillite (Aveyron, France) with hyperalkaline fluids: batch experiments performed with powdered and/or compact materials, Physics and Chemistry of the Earth 32 (2007) 320–333.
[7] F. Claret, A. Bauer, T. Schafer, L. Griffault, B. Lanson, Experimental Investigation of the interaction of clays with high-pH solutions: a case study from the Callovo–Oxfordian formation, Meuse-Haute Marne underground laboratory (France), Clays and Clay Minerals 50 (2002) 633–646.
[8] M. Adler, U.K. Mäder, H.N. Waber, High pH alteration of argillaceous rocks: an experimental study, Schweizerische Mineralogische und Petrographische Mitteilungen 79 (1999) 445–454.
[9] J.A. Chermak, Low temperature experimental investigation of the effect of high pH NaOH solutions on the Opalanius Shale, Switzerland, Clay Mineral Bulletin 40 (1992) 650–658.
[10] J.A. Chermak, Low temperature experimental investigation of the effect of high pH KOH solutions on the Opalanius Shale, Switzerland, Clays and Clay Minerals 41 (1993) 365–372.
[11] D. Savage, K. Bateman, P. Hill, C. Hughes, A. Milodowski, J. Pearce, E. Rae, C. Rochelle, Rate and mechanism of the reaction of silicates with cement pore fluids, Applied Clay Science 7 (1992) 33–45.
[12] S. Yokoyama, Atomic force microscopy; study of montmorillonite dissolution under highly alkaline conditions, Clays and Clay Minerals 53 (2) (2005) 147–154.
[13] M.C. Braney, A. Haworth, N.L. Jefferies, A.C. Smith, A study of the effects of an alkaline plume from a cementitious repository on geological materials, Journal of Contaminant Hydrology 13 (1993) 379–402.
[14] A. Bauer, G. Berger, Kaolinite and smectite dissolution rate in high molar KOH solutions at 35 and 80 °C, Applied Geochemistry 13 (7) (1998) 905–916.
[15] E.S. Hodgkinson, C.R. Hughes, The mineralogy and geochemistry of cement/rock reactions: high-resolution studies of experimental and analogue materials, Chemical Containment of Waste in the Geosphere, 157, Geological Society, London, Special Publications, 1999, pp. 195–211.
[16] O. Cuisinier, F. Masrouri, M. Pelletier, F. Villieras, R. Mosser-Ruck, Microstructure of a compacted soil submitted to an alkaline PLUME, Applied Clay Science 40 (2008) 159–170.
[17] O. Karnland, S. Olsson, U. Nilsson, P. Sellin, Experimentally determined swelling pressures and geochemical interactions of compacted Wyoming bentonite with highly alkaline solutions, Physics and Chemistry of the Earth 32 (2007) 275–286.
[18] T. Melkior, D. Mourzagh, S. Yahiaoui, D. Thoby, J.C. Alberto, C. Brouard, N. Michau, Diffusion of an alkaline fluid through clayey barriers and its effect on the diffusion properties of some chemical species, Applied Clay Science 26 (2004) 99–107.
[19] T. Melkior, S. Yahiaoui, D. Thoby, S. Motellier, V. Barthès, Diffusion coefficients of alkaline cations in Bure mudrock, Physics and Chemistry of the Earth 32 (2007) 453–462.
[20] R. Mosser-Ruck, M. Cathelineau, Experimental transformation of Na, Ca-smectite under basic conditions at 150 °C, Applied Clay Science 26 (2004) 259–273.
[21] S. Nakayama, Y. Sakamoto, T. Yamaguchi, M. Akai, T. Tanaka, T. Sato, Y. Iida, Dissolution of montmorillonite in compacted bentonite by highly alkaline aqueous solutions and diffusivity of hydroxide ions, Applied Clay Science 27 (2004) 53–65.
[22] R. Push, H. Zwahr, R. Gerber, J. Schomburg, Interaction of cement and smectitic clay-theory and practice, Applied Clay Science 23 (2003) 203–210.
[23] S. Ramirez, P. Vieillard, A. Bouchet, A. Cassagnabère, A. Meunier, A. Jacquot, Alteration of the Callovo–Oxfordian clay from Meuse-Haute Marne underground laboratory (France) by alkaline solution. I. A XRD and CEC study, Applied Geochemistry 20 (2005) 89–99.
[24] L. Sanchez, J. Cuevas, S. Ramirez, D.R. De Leon, R. Fernandez, R.V. Dela Villa, S. Leguey, Reaction kinetics of FEBEX bentonite in hyperalkaline conditions resembling the cement–bentonite interface, Applied Clay Science 33 (2006) 125–141.
[25] T. Yamaguchi, Y. Sakamoto, M. Akai, M. Takazawa, Y. Iida, T. Tanaka, S. Nakayama, Experimental and modeling study on long-term alteration of compacted bentonite with alkaline groundwater, Physics and Chemistry of the Earth 32 (2007) 298–310.
[26] E.C. Gaucher, P. Blanc, Cement/clay interactions — a review: experiments, natural analogues, and modelling, Waste Management 26 (2006) 776–788.
[27] D. Savage, C. Walker, R. Arthur, C. Rochelle, C. Oda, H. Takase, Alteration of bentonite by hyperalkaline fluids: a review of the role of secondary minerals, Physics and Chemistry of the Earth 32 (2007) 287–297.
[28] A. Dauzères, P. Le Bescop, P. Sardini, Physico-chemical investigation of cement pastes degradation in a clayey environment: experimental approach and preliminary modelling, In.: Concrete in Aggressive Aqueous Environments, Performance Testing and Modelling, 3–5 June 2009, Toulouse, France, RILEM Proceedings PRO 63 (1): (2009) 228–239
[29] B. Albert, Altération de matrices cimentaires par des eaux de pluie et des eaux sulfatées: approche expérimentale et thermodynamique, Thèse de doctorat, Ecole Nationale Supérieure des Mines de Saint Etienne et de l'Institut National Polytechnique de Grenoble, 2002, p. 294.
[30] S. Kamali, Moranville, S. Leclercq, Material and environmental parameter effects on the leaching of cement pastes: experiments and modelling, Cement and Concrete Research 38 (2008) 575–585.
[31] D. Planel, J. Sercombe, P. Le Bescop, F. Adenot, J.M. Torrenti, Long term performance of cement paste during combined calcium leaching-sulfate attack: kinetics and size effect, Cement and Concrete Research 36 (2006) 137–143.
[32] F. Badouix, Modélisation de l'altération à long terme des bétons : prise en compte de la carbonatation, Thèse de doctorat de l'Ecole Nationale Supérieure de Cachan, 2000.
[33] I. Kurashige, M. Hironaga, K. Niwase, Effects of hydrogencarbonate and chloride in groundwater on leaching of cementitious materials, CONSEC'07 Tours, 2007, pp. 615–622.
[34] L. De Windt, F. Marsal, E. Tinseau, D. Pelligrini, Reactive transport modeling of geochemical interactions at a concrete/argillite interface, Tournemire site (France), Physics and Chemistry of the Earth 33 (2008) 295–305.
[35] L. De Windt, D. Pellegrini, J. Van der Lee, Coupled modeling of cement/claystone interactions and radionuclide migration, Journal of Contaminant Hydrology 68 (2004) 165–182.
[36] Ph. Montarnal, C. Mügler, J. Colin, M. Descostes, A. Dimier, E. Jacquot, Presentation and use of a reactive transport code in porous media, Physics and Chemistry of the Earth 32 (2007) 507–517.
[37] E.C. Gaucher, P. Blanc, J.M. Matray, N. Michau, Modeling diffusion of an alkaline plume in a clay barrier, Applied Geochemistry 19 (2004) 1505–1515.
[38] D. Savage, D. Noy, M. Mihara, Modelling the interaction of bentonite with hyperalkaline fluids, Applied Geochemistry 17 (2002) 207–223.
[39] P. Vieillard, S. Ramirez, A. Bouchet, A. Cassagnabère, A. Meunier, E. Jacquot, Alteration of the Callovo–Oxfordian clay from Meuse-Haute Marne Underground Laboratory (France) by alkaline solution: II. Modelling of mineral reactions, Applied Geochemistry 19 (2004) 1699–1709.
[40] D. Savage, C.A. Rochelle, Modelling reactions between cement pore fluids and rock: implication for porosity change, Journal of Contaminant Hydrology 13 (1993) 365–378.
[41] J.M. Soler, Reactive transport modeling of the interaction between a high-pH plume and a fractured marl: the case of Wellenberg, Applied Geochemistry 18 (2003) 1555–1571.
[42] R. Push, Chemical interaction of clay buffer materials and concrete, SKBF/KBS, Report No. SFR 82-01, 1982.
[43] S. Ramirez, J. Cuevas, R. Vigil, S. Leguey, Hydrothermal alteration of «La Serrata» bentonite (Almeria, Spain) by alkaline solutions, Applied Clay Science 21 (2002) 257–269.
[44] R. Fernandez, M. Rodriguez, R.V. de la Villa, J. Cuevas, Geochemical constraints on the stability of zeolites and C–S–H in the high pH reaction of bentonite, Geochimica et Cosmochimica Acta 74 (2010) 890–906.
[45] R.V. de la Villa, J. Cuevas, S. Ramirez, S. Leguey, Zeolite formation during the alkaline reaction of bentonite, European Journal of Mineralogy 13 (2001) 635–644.
[46] A. Bouchet, A. Casagnabère, J.C. Parneix, Batch experiments: results on MX80, in: N. Michau (Ed.), Ecoclay II: Effect of Cement on Clay Barrier Performance Phase II, Final Report, ANDRA, 2004, European contract FIKW-CT-2000-0028.
[47] S. Diamond, E.B. Kinter, Adsorption of calcium hydroxyde by montmorillonite and kaolinite, Journal of Colloïd and Interface Science 22 (1965) 240–249.
[48] D.D. Eberl, B. Velde, T. McCormick, Synthseis of illite–smectite from smectite at earth surface temperatures and high pH, Clay Minerals 28 (1993) 49–60.
[49] A. Inoue, Potassium fixation by clay minerals during hydrothermal treatment, Clays and Clay Minerals 31 (1983) 81–91.
[50] N.L. Jefferies, C.J. Tweed, S.J. Wiseby, The effects of change in pH within a clay surrounding a cementitious repository, in: M. Apted, R.F. Westermann (Eds.), Scientific Basis for Nuclear Waste Management, 11, Materials Research Society, 1988, pp. 43–52.
[51] R.W. Lentz, W.D. Horst, J.O. Uppot, The permeability of clay to acidic and caustic permeants, in: A.I. Johnson, R.K. Froebel, N.J. Cavalli, C.B. Petterson (Eds.), Hydraulic barriers in soil and rock, 874, American Society for Testing and Materials. ASTM STP, 1985, pp. 127–139.
[52] M.L. Rozalen, F.J. Huertas, P.V. Brady, J. Cama, S. Garcia-Palma, J. Linarez, Experimental study of the effect of pH on the kinetics of montmorillonite dissolution at 25 °C, Geochimica et Cosmochimica Acta 72 (2008) 4224–4253.
[53] J.H.P. Van Aardt, S. Visser, Formation of hydrogarnets: calcium hydroxyde attack on clays and feldspars, Cement and Concrete Research 7 (1977) 39–44.
[54] Milodowski, A.E.; Hyslop, E.K.; Khoury, H.; Hugues, C.; Mäder, U.K.; Griffault, L.; Trotignon, L., Mineralogical alteration by hyperalkaline groundwater in northern Jordan, In: Proceedings of the Tenth International Symposium on Water–Rock Interaction, Balkema : (2001) 1347–1350
[55] D. Savage, S. Benbow, C. Watson, H. Takase, K. Ono, C. Oda, A. Honda, Natural systems evidence for the alteration of clay under alkaline conditions: an example from Searles Lake, California, Applied Clay Science 47 (2010) 72–81.
[56] M. Elie, P. Faure, R. Michels, P. Landais, L. Griffault, L. Mansuy, L. Martinez, Effect of water-cement solutions on the composition of organic compounds leached from

oxidized Callovo–Oxfordian argillaceaous sediment, Applied Clay Science 26 (2004) 309–323.
[57] T. Yamaguchi, Y. Mitsumoto, M. Kadowaki, S. Hoshino, T. Maeda, T. Tanaka, S. Nakayama, F. Marsal, D. Pellegrini, Verification of a reactive transport model for long-term alteration of cement–clay systems based on laboratory experiments and in-situ observations, CEA — JAEA meeting, 2009.
[58] E. Gaucher, C. Lerouge, Caractérisation géochimique des forages PAC et nouvelles modélisations THERMOAR, BRGM, 2007.
[59] J.-P. Girard, C. Flehoc, E. Gaucher, Stable isotope composition of CO_2 outgassed from cores of argillites: a simple method to constrain [delta]18O of porewater and [delta] 13C of dissolved carbon in mudrocks, Applied Geochemistry 20 (2005) 713–725.
[60] E.C. Gaucher, P. Blanc, F. Bardot, G. Braibant, S. Buschaert, C. Crouzet, A. Gautier, J.-P. Girard, E. Jacquot, A. Lassin, G. Negrel, C. Tournassat, A. Vinsot, S. Altmann, Modelling the porewater chemistry of the Callovian–Oxfordian formation at a regional scale, Comptes Rendus Geosciences 338 (2006) 917–930.
[61] C. Gallé, H. Peycelon, P. Le Bescop, Effect of an accelerated chemical degradation on water permeability and pore structure of cement-based materials, Advances in Cement Research 16 (3) (2004) 105–114 pp.
[62] C. Imbert, G. Touze, Mesure de la pression de gonflement et de la perméabilité de l'argilite de Meuse/Haute-Marne remaniée, 2005 NT CEA DPC/SCCME 05-309-A.
[63] A. Le Bail, http://www.sdpd.univ-lemans.fr/powdif/low_fwhmand_rp.html personal site.
[64] C.A. Reiss, The RTMS technology: dream or reality, Panalytical interne communication, CPD newsletter 27, 2002.
[65] G. Le Saoût, T. Füllmann, V. Kocaba, K.L. Scrivener, Quantitative study of cementitious materials by X-ray diffraction/Rietveld analysis using an external standard, ICC Montreal, 2008 12 p.
[66] F. Brunet, Ph. Bertani, Th. Charpentier, A. Nonat, J. Virlet, Application of 29 Si homonuclear and 1H-29Si heteronuclear NMR correlation to structural studies of calcium silicate hydrates, Journal of Physical Chemistry B 108 (2004) 15494–15502.
[67] A. Nonat, X. Lecoq, NMR Spectroscopy of Cement Based Materials, Springer, Berlin, 1998, p. 197.
[68] D. Heidmann, W. Wieker, NMR Spectroscopy of Cement Based Materials, Springer, Berlin, 1998, p. 169.
[69] I. Klur, B. Pollet, J. Virlet, A. Nonat, NMR Spectroscopy of Cement Based Materials, Springer, Berlin, 1998, p. 119.
[70] A. Nonat, The structure and stoichiometry of C–S–H, Cement and Concrete Research 34 (2004) 1521–1528.
[71] N. Marty, C. Tournassat, A. Burnol, E. Giffaut, E. Gaucher, Influence of reaction kinetics and mesh refinement on the numerical modelling of concrete/clay interactions, Journal of Hydrology 364 (2009) 58–72.
[72] A. Atkinson, The time dependence of pH within a repository for radioactive waste disposal, AERE R-11777, 1985.
[73] L. Trotignon, V. Devallois, H. Peycelon, C. Tiffreau, X. Bourbon, Predicting the long term durability of concrete engineered barriers in a geological repository for radioactive waste, Physics and Chemistry of the Earth 32 (2007) 259–274.